20th IMEKO TC10 Conference
"Measurement for Diagnostics, Optimization and Control to Support Competitiveness and Innovation"
Lisbon, Portugal, September 28–29, 2026

Anomaly detection of ventilation fan by training a variational auto-encoder with current waveforms of brushless DC motor

Yukio Hiranaka[1,2], Koichi Tsujino[2]

Ojiro Miyazaki[3], Tadashi Yasufuku[3], Fumiaki Tsukazaki[3], Kazuyuki Kouno[3]

[1]Hiranaka Technology Research, Susono, Japan
[2]AiSpirits, Tokyo, Japan
[3]Nuvoton Technology Corporation Japan, Kyoto, Japan

***Abstract* – Anomalies in motor-driven equipment can be detected potentially by measuring the current of the driving motor. We attempt to utilize unsupervised learning of motor current to detect load fluctuations and bearing anomalies in ventilation fans. By training a variational auto-encoder on the cyclic current waveforms of a motor under normal conditions, anomalies—such as deviations in cycle length, peak current, and waveform patterns—can be detected using anomaly scores derived from latent variables. This approach is applied to experimental data from a small brushless DC motor used in a ventilation fan to verify its effectiveness.**

Keywords – Anomaly Score, Motor Current, Ventilation Fan, Variational Auto-Encoder, Industry Innovation and Infrastructure.

I. INTRODUCTION

Detecting anomalies in equipment is crucial for condition-based maintenance and is expected to have applications in various fields. In particular, motor-driven equipment often operates for a long period of time, and any failure may force the equipment to shut down. Therefore, detecting equipment anomalies at an early stage is desirable. This study presents an anomaly detection method for ventilation fans driven by brushless DC motors by monitoring current waveforms using a variational auto-encoder (VAE) [1]. Specific methods and illustrating results are presented.

II. RELATED STUDIES IN THE LITERATURE

Various methods exist for detecting anomalies in rotating machinery, and most of them focus on spectral analysis of vibrations [2]. However, vibrations involve many factors that complicate analysis, such as resonance and harmonics. A more reliable approach with a clearer causal relationship is the analysis of the motor's current waveform. In this case, however, determining which waveform features to focus on becomes critical [3,4,5].

Also, when input information is multidimensional, it is necessary to extract appropriate information that represents the anomalous state, and the choice of information compression method greatly affects the results. While effective features were traditionally selected through manual human analysis, recent AI-based methods have enabled the efficient extraction of comprehensive information directly from the data. As there are various types of anomalies, the characteristics of "anomalies" cannot be identified from the beginning, a suitable learning method is required that makes judgments based on existing information. Among various AI techniques, VAEs are particularly promising for their ability to extract essential latent variables from the distribution of normal data [6].

III. DESCRIPTION OF THE METHOD

A. Raw motor current

When measuring the current flowing through the power line of a single-phase brushless DC fan (SanAce80 9GA0812P6G001, 80x80x20mm, PWM speed controllable), the current is observed to switch ON/OFF according to the PWM signal as shown in Fig. 1.

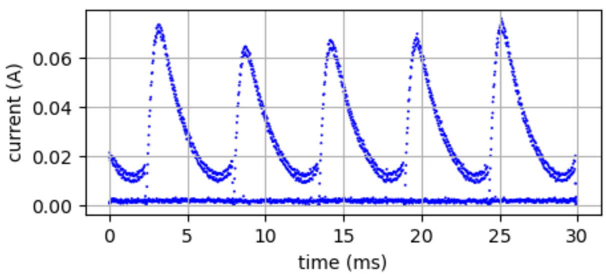

Fig. 1. Example of the motor current for 40% PWM rate.

Since the current changes depending on the observation timing, a clear set of cyclic waveforms can be obtained by taking only the maximum current from each PWM cycle as the representative value (Fig. 2).

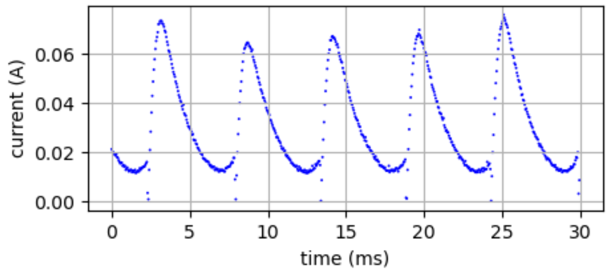

Fig. 2. Trace of maximum current value of each PWM cycle.

B. Maximum current cycle waveform

The motor consists of four outer rotor poles, resulting in four current cycles per revolution. These cycles exhibit the fluctuations in peak current values observed in Fig. 2. For precise anomaly detection, it is necessary to determine which cycle waveform to use for anomaly detection. To isolate the current waveform for each rotor pole, the second-order difference of the data in Fig. 2 is calculated. The resulting local maxima are defined as the endpoints of each cycle, as indicated by the orange crosses in Fig. 3.

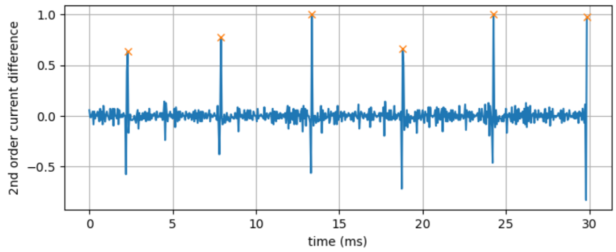

Fig. 3. Second order difference of Fig.2.

From the current waveform of at least four consecutive cycles, the cycle in which the peak current value is higher than the others is extracted and taken out as the maximum current cycle waveform (Fig. 4).

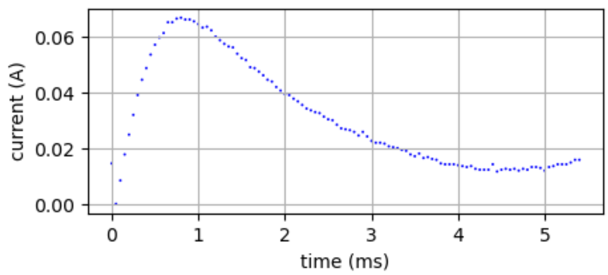

Fig. 4. Example of the maximum current cycle.

C. Rise time alignment

The start of the current cycle depends on the rotational state and does not coincide with the current sampling timing. Therefore, the starting point of the obtained current cycle fluctuates by about one PWM cycle. To eliminate this fluctuation, sampling timing correction was performed by linear interpolation of the current data, as shown in Fig. 5.

Specifically, the starting point for each cycle is synchronized to a predefined current level (START_LVL = 0.05 A), with its precise location calculated using an internal division ratio (a:b) between sampling points. The interpolated current values (red circles) for each PWM period are aligned with the starting value and used as training data and test data for anomaly score calculation.

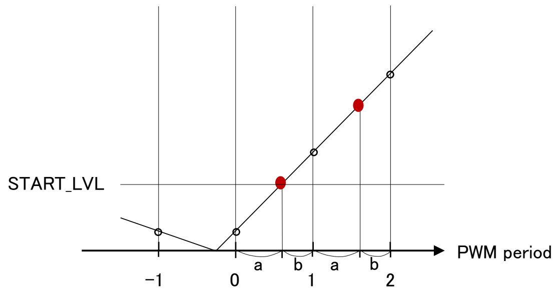

Fig. 5. Rise time alignment by linear interpolation.

D. VAE anomaly score

Similar to the anomaly detection using vibrational frequency spectra [6], a VAE is trained to form the latent spatial distribution of the training data to follow a standard normal distribution. The anomaly score can be calculated as the normalized Euclidean distance from the center of the normal distribution.

Specifically, as shown in equation (1), the deviation of the latent value z_i on i axis of the VAE latent space (D dimensions) from the mean $\overline{z_i}$ is corrected by the variance σ_i, which corresponds to the normalized distance from the distribution center and is taken as the anomaly score V_D. However, when the number of dimensions is redundant, this score is overestimated, so it is corrected by Dcmps, which represents the redundancy obtained by equations (2) and (3).

$$V_D = \sqrt{\frac{1}{D_{cmps}} \sum_{i=1}^{D} \left(\frac{z_i - \overline{z_i}}{\sigma_i}\right)^2}, \tag{1}$$

$$D_{cmps} = \frac{1}{D} \sum_{i=1}^{D} \sum_{j=1}^{D} R^2(f_i, f_j), \tag{2}$$

$$R(f_i, f_j) = \frac{1}{N} \sum_{n=1}^{N} f_i(n)\, f_j(n), \tag{3}$$

where $f_i(n)$ is the input basis function corresponds to the i-th latent variable = 1, N is the number of input variables, and $R(f_i, f_j)$ represents the correlation of two basis functions.

Figure 6 shows the structure and training flow of the VAE, where the encoder compresses the input variables to latent variables of D dimensions.

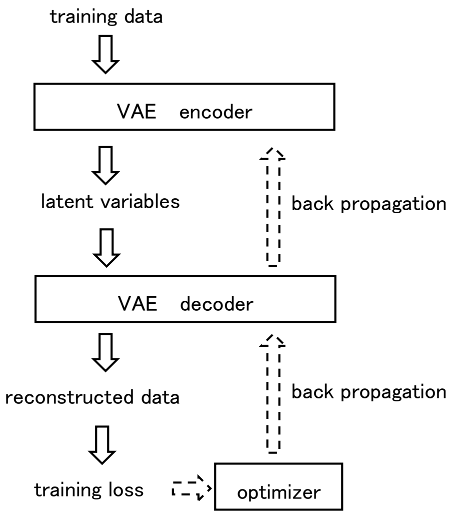

Fig. 6. Processing flow of the VAE.

As shown in Fig. 4, the current cycle waveform had over 100 points, so the input variable was set to 100, the VAE had a 3-layer structure with 16 units in the hidden layer, the activation function was linear, the optimization algorithm was Adam, the mini-batch size was 1, and the training iterations were 1,000.

The latent space dimensionality D was set to three, because there were cases where anomalies could not be separated in two dimensions but could be separated in three dimensions. Depending on the situation of the subject, differences can be observed in the peak value, peak time, and tail value of the current waveform at least, so the selection of three dimensions is considered suitable.

IV. RESULTS AND DISCUSSIONS

The training data was the maximum current cycle waveform under normal conditions (no particular load applied) shown in Fig. 7. When the airflow was restricted by inserting a shielding material downflow, the tail current increased slightly (Fig. 8).

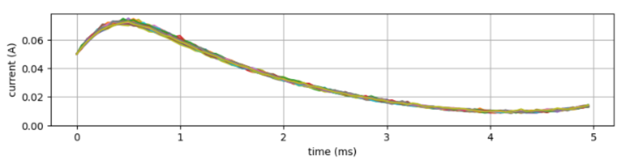

Fig. 7. Examples of normal state current.

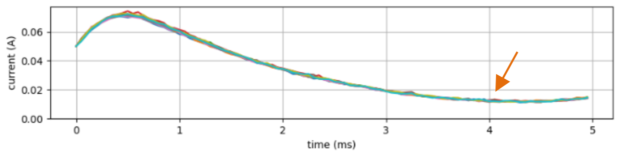

Fig. 8. Examples of anomalous state current.

Figure 9 shows the latent space distribution (shown as a three-view diagram due to its three-dimensionality) obtained by inputting the data from Figures 7 and 8 into the VAE encoder trained on the data in Figure 7. The blue points correspond to the training data in Figure 7, and the green points correspond to the anomalous data in Figure 8. The training data and anomalous data are clearly separated.

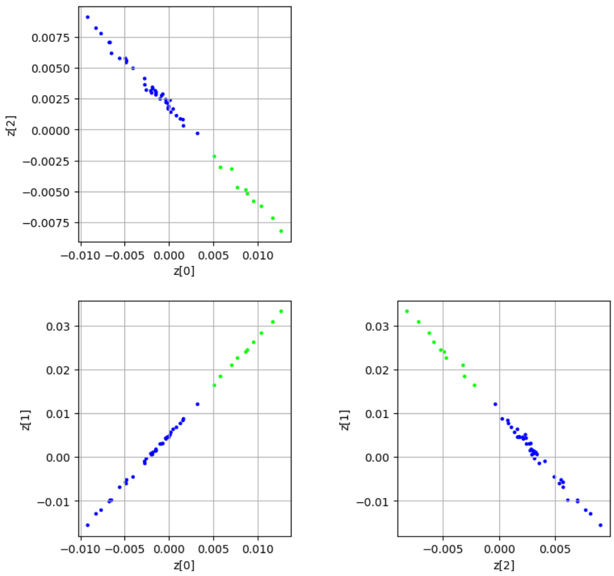

Fig. 9. Three dimentional latent space distribution.

In the anomaly score plot (Fig. 10), the scores for the normal training data (blue) remain below 3, which corresponds to three times the standard deviation of the normal distribution. In contrast, the anomalous data (green) exhibit significantly higher values, indicating a clear deviation from the normal state.

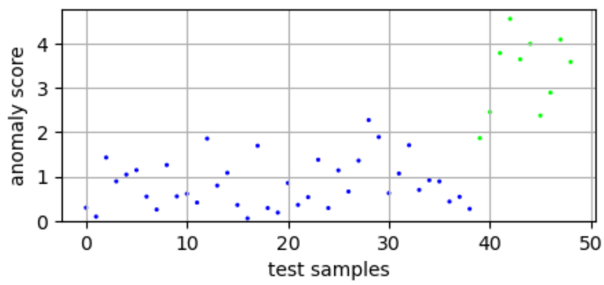

Fig. 10. Anomaly scores for normal(blue) and anomalous(green) states.

In this example, an increase in tail current due to the load is detected as an anomaly. However, other variations—such as decreased current levels, shifts in cycle length, or deformations in the waveform—also result in higher anomaly scores. This is because any deviation from the normal current pattern causes the data to fall outside the learned latent distribution, enabling the detection of various anomalous states. Future work will focus on verifying the detection performance across a wider range of failure modes.

V. CONCLUSION

This study demonstrated that anomalous fan state can be detected by measuring the motor current waveform. Specifically, the method enables robust anomaly detection by extracting peak current values for each PWM cycle, isolating individual cycles to mitigate the influence of magnetic pole configurations, correcting sampling fluctuations via linear interpolation, and finally, computing anomaly scores through a VAE.

REFERENCES

[1] **Kingma D.P.; Welling M.:** Auto-Encoding Variational Bayes, Proc. International Conference on Learning Representations, arXiv:1312.6114, 2014.

[2] **Randall, R.B.:** Vibration-based Condition Monitoring: Industrial, Aerospace and Automotive Applications, Wiley, 2ndEd, 2021.

[3] **Dhomad, T,A.; Jabar A.A.:** Bearing Fault Diagnosis Using Motor Current Signature Analysis and the Artificial Neural Network, International Journal on Advanced Science Engineering Information Technology, vol.10, no.1, pp.70-79, 2020.

[4] **Ebrahimi, B.M.; Roshtkhari M.J.; Faiz J.; Khatami S.V.:** Advanced Eccentricity Fault Recognition in Permanent Magnet Synchronous Motors Using Stator Current Signature Analysis, IEEE trans. Industrial Electronics, vol.61, no.4, pp.2041-2052, 2014.

[5] **Benbouzid M.E.H.:** A Review of Induction Motors Signature Analysis as a Medium for Faults Detection, IEEE trans. Industrial Electronics, vol.47, no.5, pp.984-993, 2000.

[6] **Hiranaka Y.; Tsujino K.:** VAE Deviation for Detecting Bearing Anomalies, 17th IMEKO TC 10 and EUROLAB Virtual Conference, October 20-22, 2020.